Tissue Factor Signals Airway Epithelial Basal Cell Survival via Coagulation and Protease-Activated Receptor Isoforms 1 and 2

Shama Ahmad[1,2], Aftab Ahmad[1,2], Raymond C. Rancourt[1,2], Keith B. Neeves[3], Joan E. Loader[1,2], Tara Hendry-Hofer[1,2], Jorge Di Paola[4], Susan D. Reynolds[1]*, and Carl W. White[1,2]*

[1]Department of Pediatrics, National Jewish Health, Denver; [2]Department of Pediatrics, and [4]Human Medical Genetics Program, University of Colorado, Denver, Colorado; and [3]Department of Chemical and Biological Engineering, Colorado School of Mines, Golden, Colorado

Tissue factor (TF) initiates the extrinsic coagulation cascade and is a high-affinity receptor for coagulation factor VII. TF also participates in protease-activated receptor (PAR)1 and PAR2 activation. Human epithelial basal cells were previously purified on the basis of TF expression. The purpose of this study was to determine if tracheobronchial epithelial basal cell–associated TF drives coagulation and/or activates PARs to promote basal cell functions. We used human tracheobronchial tissues to isolate human airway epithelial cells using specific cell surface markers by flow cytometry and studied TF expression by immunostaining. TF-dependent fibrin network formation was observed by confocal and scanning electron microscopy. TF knockdown was done using short hairpin RNA, and TF mRNA was measured using quantitative RT-PCR. We found that 97 ± 5% of first-passage human tracheobronchial epithelial cells were basal cells, and 100% of these basal cells expressed TF. Basal cell–associated TF was active, but TF activity was dependent on added extrinsic coagulation cascade factors. TF inhibition caused basal cell apoptosis and necrosis. This was due to two parallel but interdependent TF-regulated processes: failure to generate a basal cell–associated fibrin network and suboptimal PAR1 and PAR2 activity. The data indicate that membrane surface TF mediates airway epithelial basal cell attachment, which maintains cell survival and mitotic potential. The implications of these findings are discussed in the context of basal cell–associated TF activity in normal and injured tissues and of the potential for repair of airway epithelium in lung disease.

Keywords: tissue factor; epithelium; clotting; fibrin; tracheobronchial

CLINICAL RELEVANCE

Although tissue factor (TF) has been previously localized to the basal cell region of airways, the role of TF activity in tracheobronchial epithelial basal cell function is unknown. TF activity on the surface of tracheobronchial epithelial basal cells causes fibrin formation, leading to provisional matrix formation, basal cell attachment, survival, and proliferation. We demonstrate that TF activity is essential for airway epithelial repair after injury.

Tissue factor (TF) is a transmembrane cell receptor and cofactor for factor VII (FVII) and serves biological functions beyond its established role in blood coagulation (1). TF may act as a transmembrane signaling molecule by activating and delivering coagulation factors for signaling, and the TF-coagulation FVIIa complex activates G protein–coupled receptors, including the protease-activated receptors (PARs) (2). Under pathologic conditions, TF can be expressed by circulating blood elements (monocytes, neutrophils, and platelets) and by an associated elevated number of cell-derived circulating microparticles. The role of TF in epithelial cell function is much less well understood than its role in the circulation and in hemostasis.

In acute lung injury, increased coagulation and decreased fibrinolysis result in diffuse alveolar fibrin deposition, potentially increasing lung inflammation (3). Recent evidence indicates that the damaged alveolar epithelium expresses TF (4) and that FVII-activating protein expression is increased (5). Alveolar procoagulant microparticles are also elevated (6), and intrinsic elevation of tissue factor pathway inhibitor (TFPI) expression is insufficient to inhibit this procoagulant effect (7). Coagulation pathologies also occur in conducting airways. For example, the sulfur mustard analog 2-chloroethyl-ethylsulfide causes production of fibrin-rich, airway-occlusive casts after acute inhalation (8), and the TF pathway is activated in this process (9). Fibrin cast formation in proximal airways also occurs in burns and in smoke inhalation, with postextubation airway injuries, and in children with congenital heart disease (post-Fontan procedure) (10, 11). Thus, excessive fibrin formation by TF pathway activation can occur throughout airways, potentially causing obstructive and fibrotic pathologies.

Despite its role in tissue damage, TF and its activation of coagulation may have protective functions. Coagulation and fibrin deposition in wounds or other sites of injury (e.g., skin) is critical to maintain epithelial barrier integrity and to protect against invading microbes. Recently, low TF–expressing mice demonstrated delayed wound healing, difficulty in responding to infection, and the potential for pathologic bleeding (12). Inactivation of the TF gene or the gene encoding its endogenous inhibitor (i.e., TFPI) causes embryonic lethality (13). Thus, TF may provide a homeostatic envelope that protects organisms against bleeding after injury (14, 15).

The normal bronchial epithelium maintains a barrier against inhaled harmful agents by efficiently and rapidly repairing

(*Received in original form May 24, 2012 and in final form September 17, 2012*)

* These authors contributed equally to this work.

This work was supported by National Institutes of Health grants RC1HL099461 (S.D.R. and C.W.W.), R01-ES014448 (C.W.W.), and KL2RR025779 (S.A.) and by the CounterACT Program, National Institutes of Health, Office of the Director, and the National Institute of Environmental Health Sciences grant U54 ES015678 (C.W.W.). Foundation support was received from Max and Yetta Karasik Family Foundation (C.W.W.) and by American Heart Association grant 0830418N (A.A). Imaging experiments were performed in the University of Colorado Anschutz Medical Campus Advanced Light Microscopy Core, which is supported in part by National Institutes of Health/NCRR Colorado CTSI grant UL1 RR025780.

Author Contributions: Concept and design: A.A., S.A., S.D.R., and C.W.W.; analysis and interpretation: A.A., S.A., R.C.R., K.B.N., J.E.L., T.H.H., J.D.P., S.D.R., and C.W.W.; manuscript preparation: S.A., S.D.R., and C.W.W.

Correspondence and requests for reprints should be addressed to Shama Ahmad, Ph.D., Department of Pediatrics, Pediatric Airway Research Center, Mailstop 8615, P15-4016, University of Colorado Denver, 12700 E. 19th Ave, Aurora, CO 80045. E-mail: shama.ahmad@ucdenver.edu

This article has an online supplement, which is accessible from this issue's table of contents at www.atsjournals.org

Am J Respir Cell Mol Biol Vol 48, Iss. 1, pp 94–104, Jan 2013

Originally Published in Press as DOI: 10.1165/rcmb.2012-0189OC on October 11, 2012
Internet address: www.atsjournals.org

affected areas. Epithelial wounding exposes the basement membrane and extracellular matrix and causes TF activation (16). TF is expressed by airway epithelial basal cells (16–18) andhas been used as a marker for basal cell isolation and purification (16, 18). Fibrin formation may be required for repair in airway epithelial cell lines (19). We have demonstrated that human airway epithelial basal cells use cell surface TF to form fibrin networks on their surface and that this fibrin network formation was critical for their survival. We also established a role for TF in PAR activation and showed that this activity enhanced basal cell survival and proliferation. Together, these findings suggest that TF activity may be a critical component of the epithelial repair process.

MATERIALS AND METHODS

Human Airway Epithelial Cell Isolation

Human tracheobronchial tissue was procured from National Disease Research Interchange under National Jewish Institutional Review Board–approved protocols. Cell harvest and culture were performed using established procedures (20). Briefly, epithelial cells were removed from lower trachea and bronchi by protease XIV digestion and plated in bronchial epithelial growth medium on collagen-coated dishes.

Fluorescence-Activated Cell Sorting Analysis

One million passage 1 cells were incubated with anti–TF-FITC (American Diagnostica, Stamford, CT), anti-CD31-APC (eBioscience, San Diego CA) (to exclude endothelial cells), anti–CD45-APC (eBioscience) (to exclude hematopoietic cells), and anti–CD90-APC (eBioscience) (to exclude fibroblasts) antibodies diluted in PBS containing BSA (1%) for 30 minutes at 4°C. Nonimmune IgG1κ-APC and IgG1-FITC were used as isotype controls. Cells were washed twice and suspended in PBS-BSA. The DNA-intercalating dye 7-aminoactinomycin D (7-AAD) was added to stain dead cells. Cell sorting was performed with a Moflo-XDP high-speed cell sorter (Beckman Coulter, Brea, CA) equipped with a CyCLONE automated cloner. Compensation for spectral overlap was done using single-color positive and negative compensation beads (BD Biosciences, San Jose, CA). Gates were set according to unstained and isotype controls. Doublets were excluded by side scatter versus forward scatter (FS) and FS-INT area versus FS dot plots. Cell count versus 7-AAD plot defined dead cells. TF-positive basal cells were then sorted at a rate of 5,000 events per second. Sorted cells were reanalyzed for purity and viability.

TF Knockdown

Knockdown of TF was performed using lentiviral-mediated short hairpin RNA (shRNA) (Sigma, St. Louis, MO) transduction as described previously (21). The details of RT-PCR to quantify mRNA are provided in the online supplement.

Confocal Microscopy

Cells were cultured on collagen-coated coverslip chamber slides. Thirty minutes before imaging, FITC-labeled fibrinogen was added (22). Confocal imaging was performed as described previously (8, 23). A two-photon LSM 510 confocal microscope (Zeiss, Thornwood, NY) was used to obtain images and Z-stacks.

Scanning Electron Microscopy

Human airway epithelial basal cells were cultured at approximately 10,000 cells/cm^2 on 14-mm coverslips. Twenty-four hours later, treatments were performed, and cells were fixed in 2.5% glutaraldehyde in 0.1 M sodium cacodylate buffer (pH 7.4) for 4 hours, rinsed four times, and stored in 0.1 M sodium cacodylate buffer (pH 7.4). Samples were dehydrated in graded ethanol solutions (50%, 70%, 80%, 90%, 100%, and 100%) for 5 minutes each and chemically dried once in 50% and then twice in 100% hexamethyldisilazane for 5 minutes each time. Samples were air dried overnight at room temperature in a desiccator. A thin film ($\sim$ 10 nm) of gold was sputtered on samples before imaging. Images were taken with an accelerating voltage of 5 KV and at a 6-mm working distance on a JEOL 7000 FE (JEOL, Peabody, MA) scanning electron microscope. Each experimental condition was imaged in 10 positions at magnifications of 2,000× and 25,000×. Brightness and contrast were adjusted on scanning electron microscopy images to optimize viewing. No other image manipulation was performed.

Statistical Analysis

ANOVA with Tukey comparisons was calculated using JMP Software (SAS, Cary, NC). $P < 0.05$ was considered statistically significant.

RESULTS

Human Tracheobronchial Airway Epithelial Cells Express TF *In Vitro*

To define TF function, we first determined if isolated human tracheobronchial airway epithelial cells (HAECs) expressed this marker. HAECs were isolated from tracheas and bronchi of patients dying from nonlung disease (20). Passage 1 HAECs were harvested at 80% confluence. Immunostaining indicated that the majority expressed TF (*see* Figure E1A in the online supplement). Next, TF expression was quantified in passage 1 HAECs using flow cytometry. An iterative gating strategy (Figure 1A) was used. Dead cells were excluded by 7-AAD staining, and nonepithelial cells (hematopoietic cells, endothelial cells, and fibroblasts) were excluded by CD45, CD31, and CD90 staining (Figure 1A). TF expression on live epithelial cells was present in 97 ± 5% ($n = 14$ donors) (Figure 1B). TF fluorescence intensity was uniformly distributed about the mean, indicating that TF positivity defined a single cell population.

To determine the phenotype of live/epithelial/TF+ cells, cytospin preparations were stained for cell type–specific markers. Because motile cilia can be sheared during FLOW cytometry, ciliated cells were detected by staining for γ tubulin. Basal bodies expressing this antigen are located at the terminal plate of ciliated cells and in the centrosomes of all cells. Mucus cells were detected by staining for mucins Muc5AC and Muc5B. Basal cells were detected by staining for keratin 5. All TF-positive cells expressed keratin 5 (Figure 1C). Thus, passage 1 HAECs were basal cells and are henceforth called "'basal cells."

Basal Cells Express Active TF

TF initiates clotting by interacting with Factor VII in the presence of calcium, resulting in activation of Factor X. Factor Xa then initiates conversion of prothrombin to thrombin, which converts fibrinogen to fibrin. Thus, TF activity can be evaluated using an assay detecting cleavage of a Factor X substrate (9). Initial experiments demonstrated that basal cell cultures expressed active TF. This activity was proportional to basal cell number (Figure E1B). TF activity was detected only when Factor VII and Factor X were added (Figures E1C and E1D).

To determine if Factor Xa generation was TF dependent, varying numbers of basal cells were plated at low cell density and incubated for 24 hours (Figure 1D). Cultures were then treated with an isotype-matched control antibody or polyclonal anti–TF-antibody for 30 minutes, and TF activity was assayed (Figure 1E). TF was detected in isotype IgG-treated cultures, and this activity was proportional to the number of cells plated (Figure 1E). In contrast, cultures treated with TF antibody exhibited significantly less TF activity at all cell inputs. To further evaluate TF activity, basal cells were treated with human recombinant TFPI. Vehicle-treated cultures exhibited cell-number–dependent TF activity (Figure 1F). In contrast, TFPI-treated cultures exhibited no detectable TF activity. The basal cells expressed active TF. We suggest that fibrin formed from TF activity on basal cell surface

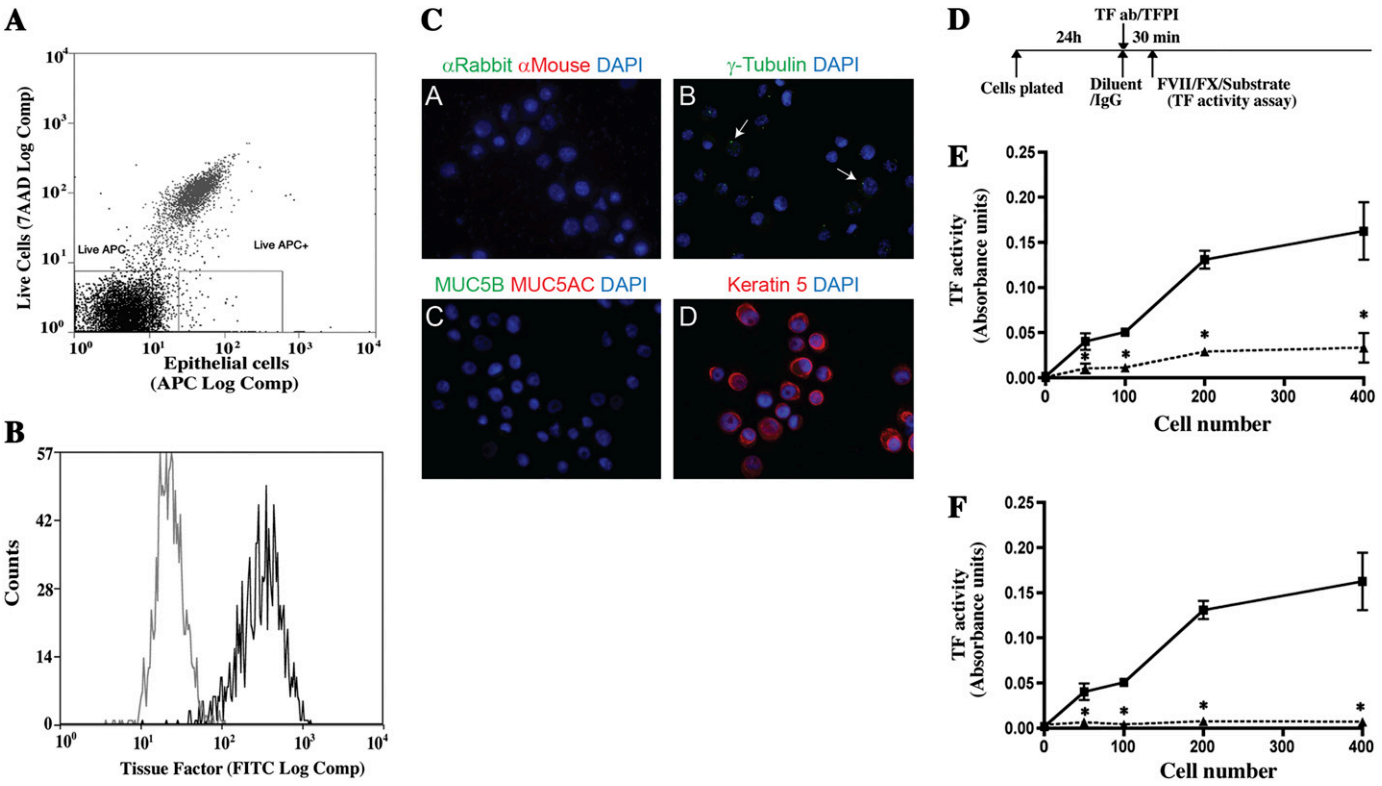

Figure 1. Human tracheobronchial basal cells (HAECs) express tissue factor (TF). Passage 1 HAECs were cultured for 5 days on collagen-coated plates as described in MATERIALS AND METHODS. Cells were harvested and stained, and fluorescence-activated cell sorting was performed. (*A*) Live cells were defined as those that excluded 7-aminoactinomycin D (7-AAD), and epithelial cells were identified as those that did not stain with allophycocyanin (APC)-tagged CD31 (endothelial cells), CD45 (hematopoietic cells), or CD90 (fibroblasts cells). (*B*) TF-positive cells were identified by comparison of live epithelial cells that were stained with an isotype control (*gray*) and FITC-conjugated TF antibody (*black*). The data represent three independent experiments performed with cells isolated from three different donors. (*C*) To determine if purified HAECs are basal cells, live, epithelial, TF+, passage 1 HAECs were recovered by flow cytometry and deposited onto microscope slides using a cytocentrifuge. Because cilia tend to be sheered during flow cytometry, γ-tubulin was used to detect basal bodies located at the terminal plate of ciliated cells. Mucus cells were detected by staining for MUC5AC and MUC5B. Basal cells were detected by staining for keratin 5 (K5, purified basal cells, differentiated epithelial cell cultures, and fixed tracheal tissues were used as positive controls). Positive controls for MUC5B and γ-tubulin were also used. Images representative of TF-positive cells from three donors are shown. (*A*) Secondary antibodies only. (*B*) γ-Tubulin (*green*). (*C*) Muc5AC (*red*) and Muc5B (*green*). (*D*) Keratin 5 (*red*). (*D*) Basal cells were allowed to adhere to collagen-coated plates for 24 hours and then treated for 30 minutes with an isotype control antibody or antitissue factor antibody or with diluent or tissue factor pathway inhibitor (TFPI). TF activity was determined by the S-2765 FXa substrate assay in the presence of Factor VII, Factor X, and $CaCl_2$. (*D*) Effect of anti-TF antibody on TF activity. *Squares*, isotype control; *triangles*, anti-TF antibody-treated cells. (*E*) Effect of TFPI treatment on TF activity. *Squares*, diluent control; *triangles*, TFPI treatment. Data are presented as mean ± SEM ($n = 6$). *$P < 0.05$ for control versus treated cultures.

serves as a cell attachment matrix. We also determined whether the collagen matrix in these cultures was capable of affecting TF-dependent FX cleavage. Collagen at concentrations used in coating the plastic tissue culture dishes (coated or in solution) did not affect TF activity (Figure E2).

TF Is Necessary for Basal Cell Survival

To determine if TF played a role in basal cell survival, TF mRNA was knocked down using shRNA technology (Figure 2A) using lentiviral vector. Treatment with TF-shRNA decreased TF mRNA (Figure 2B) and protein (Figure 2C) expression by approximately 50%.

To determine if TF knockdown promoted cell death, caspase 3/7 release was measured in supernatant from shRNA-treated cultures. This did not differ between control and nontarget shRNA-treated cells (Figure 2D). However, caspase 3/7 levels increased approximately 2-fold in TF-shRNA–treated cells. To determine if cells underwent apoptosis or necrosis, the PI/annexin V flow cytometry method was used (24). Treatment with nontarget shRNA increased apoptotic cells 1.5-fold but did not increase the necrotic cell frequency (Figure 2E). In contrast, treatment with TF-shRNA increased apoptosis and necrosis 2-fold.

Proliferation of shRNA-treated cells was measured by [^{3}H] thymidine incorporation 48 hours after shRNA treatment. The rate of proliferation did not differ between untreated and nontarget shRNA-treated cells but decreased by approximately 30% in cells treated with TF-shRNA (Figure 2F). These data indicated a direct TF effect on basal cell survival and a secondary effect on basal cell proliferation.

Active TF Is Necessary for Basal Cell Survival

To determine if TF activity was required for basal cell survival, cells adhered for 24 hours were treated with diluent or TFPI for 24 hours, and cell number was analyzed by the MTT assay (25) (Figure 2G). TFPI treatment decreased cell number by 75% at all cell inputs (Figure 2H), indicating that TF activity was necessary for basal cell survival.

To investigate the mechanism of TFPI-induced basal cell attrition, basal cells adhered for 24 hours were treated with vehicle

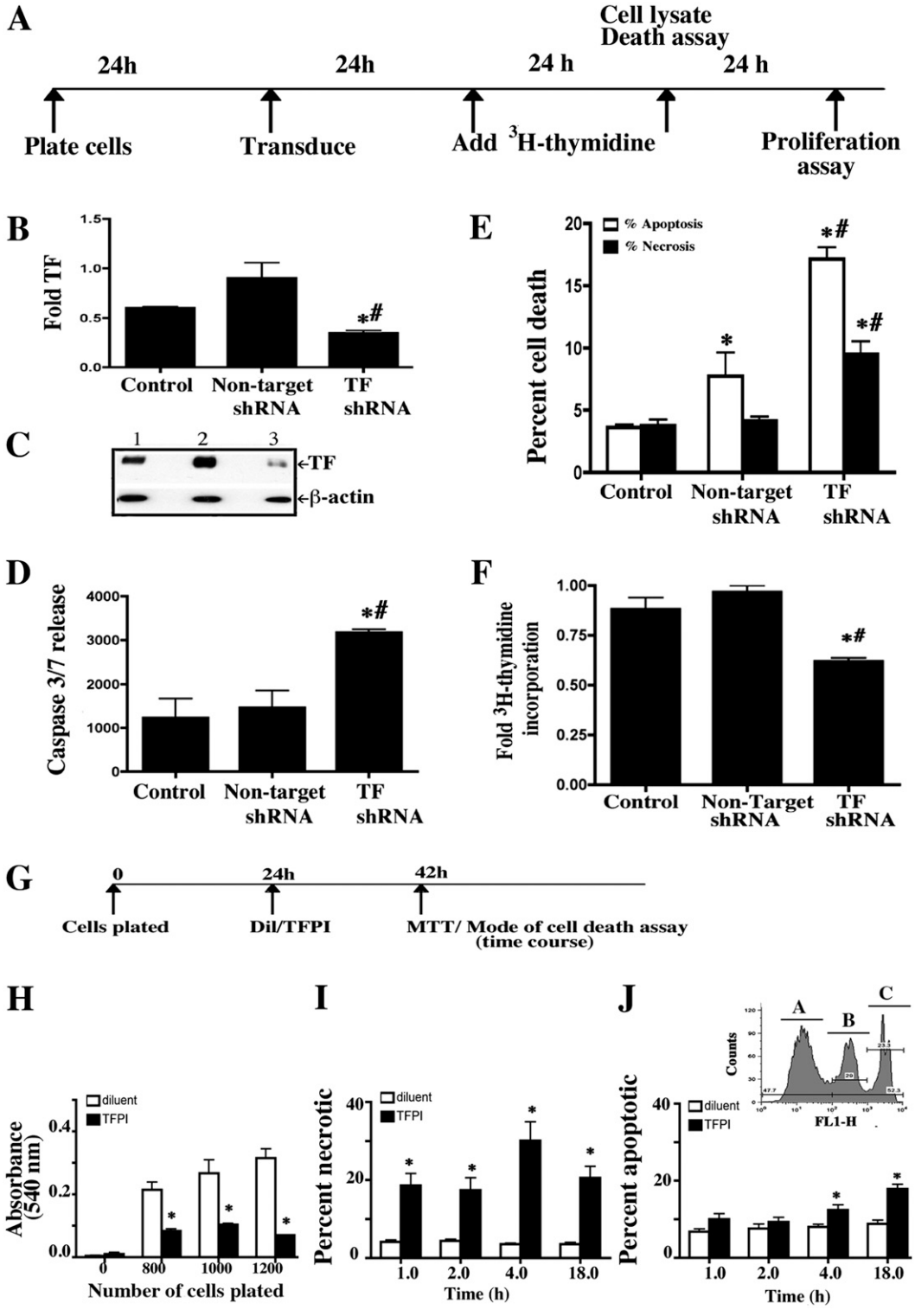

Figure 2. TF expression is necessary for basal cell survival. (*A*) Basal cells were cultured on collagen-coated plates and transduced with nontarget or TF-specific short hairpin RNA (shRNA). TF knockdown was assayed 48 hours after transduction. Cell death was assayed 48 hours after transduction, and proliferation was assayed 72 hours after transduction. (*B*) TF mRNA abundance was analyzed using quantitative real-time RT-PCR. Fold TF indicates the ratio of TF mRNA to 18 s rRNA normalized to 1 for nontarget shRNA. (*C*) Western blot analysis of TF protein abundance. *Lane 1*, nontransduced control; *lane 2*, nontarget shRNA; *lane 3*, TF-specific shRNA-transduced cells and β-actin served as the loading standard. (*D*) Caspase 3/7 activity was measured in culture medium using the Caspase-Glo 3/7 assay. Caspase 3/7 release indicates the luminescence (in relative luminescence units) with the background signal subtracted. (*E*) The mode of cell death was evaluated in attached cells and floating cells using the annexin V (apoptosis) and Sytox Green (necrosis) assay. The frequency of cells that were apoptotic (*white bar*) or necrotic (*black bar*) is presented as a percent of all cells. (*F*) Proliferation was evaluated by analysis of (^{3}H)-thymidine incorporation. Fold 3H-thymidine incorporation indicates the counts per minute for the test sample relative to nontransduced control. Each data set represents three independent experiments performed with cells isolated from three different donors. The data are presented as mean ± SEM ($n = 6$). *$P < 0.05$ relative to the nontransduced control. $^{\#}P < 0.05$ relative to the nontarget shRNA treated control. (*G*) To determine if active tissue factor is required for basal cell survival, basal cells were plated on collagen-coated plates and allowed to adhere for 24 hours. Cells were then treated with diluent or TFPI for 18 hours, and cell number, necrosis, and apoptosis were evaluated. (*H*) Cell number was evaluated using the MTT assay. (*I*) The frequency of necrotic cells was determined by Sytox green assay. (*J*) The frequency of apoptotic cells was determined by annexin V apoptosis assay. The *inset* in *I* is a flow cytometry image for analysis of alive (peak A unstained), apoptotic (peak B, Annexin FITC), and necrotic (peak C, Sytox green) cells. Each data set represents three independent experiments performed with cells isolated from three different donors. Data are presented as mean ± SEM ($n = 6$). *$P < 0.05$ relative to diluent controls. *White bar*, diluent; *black bar*, TFPI.

or TFPI and assayed for apoptosis and necrosis (Figures 2I and 2J). Treatment with TFPI increased the necrotic cell index at each time point and the apoptotic cell index at the 4- and 18-hour time points as compared with diluent, which had no effect. Similar results were obtained when cell death was assayed by caspase release or annexin binding (Figure E3). These data confirmed that TF activity was necessary for basal cell survival.

Because caspase 3 is a key enzyme of final pathway of apoptosis, to distinguish between extrinsic and intrinsic apoptotic pathway, the role of caspase 8 and 9 in TFPI-induced basal cell apoptosis was investigated. At 6 and 18 hours after TFPI treatment, caspase 8 was significantly elevated (Figure E4A). However, caspase 9 was not significantly different (not shown), indicating a major role of the extrinsic pathway.

Phosphorylation of the cytoplasmic domain may play an important role in TF-mediated cellular adhesion (26). We therefore investigated if TFPI treatment altered TF phosphorylation. TFPI treatment did not affect TF phosphorylation (Figures E4B and E4C). PARs phosphorylate the cytoplasmic domain of TF (27). PAR agonists were used as positive controls in these studies, and they did increase phosphorylation of TF.

Basal Cells Express a Subset of Clotting Cascade Components

TF initiates the extrinsic clotting cascade that requires multiple factors for propagation (28). These clotting factors may be supplied by TF-expressing cells or by the surrounding environment. Thus, we determined which clotting factors and related molecules were expressed by TF-positive basal cells. Gene expression was assayed by quantitative RT-PCR using cDNA substrate prepared from basal cells and human liver, a positive control (Figure E5A). mRNA abundance in basal cells was expressed as percentage of that in liver. Gene expression was also evaluated in scratch-wounded basal cells to determine potential coagulation factor induction by injury. Basal cells expressed high levels of TF, TFPI (Figures E5B and E5C), and fibrinogen γ chain mRNA (Figure E5H). In contrast, basal cells expressed very low levels of thrombin, antithrombin, and Factor V and X mRNA (Figure E5D–E5G). Basal cells did not express detectable Factor VII or IX mRNA (not shown). Thus, basal cells expressed an incomplete repertoire of clotting factors.

Basal Cells Form a TF-Dependent Fibrin Network on their Surface

We sought to determine how TF activity promotes basal cell survival. It is known that activation of coagulation causes formation of fibrin networks and that these networks can seal epithelial defects (14, 15). We hypothesized that fibrin networks serve as substrates for attachment of reparative cells. To test this concept, basal cells were cultured at 80% confluence on glass coverslips (submerged) or on air–liquid interfaces for 10 days. FITC-labeled fibrinogen was used to determine if fibrinogen was converted to fibrin (Figure 3A). Fibrin networks were detected 30 minutes after adding labeled fibrinogen to submerged or air–liquid interface cultures (Figure 3B, *panels B and G*). Fibrin network formations were enhanced by prothrombin, Factor VII, and Factor X (Figure 3B, *panels C and H*). The addition of TFPI decreased cell surface fibrin networks (Figure 3B, *panels D and I*), and the specific fibrin cross-linking inhibitor peptide Gly-Pro-Arg-Pro (GPRP) (29) eliminated fibrin networks (Figure 3B, *panels E and J*). Thus, basal cell–associated

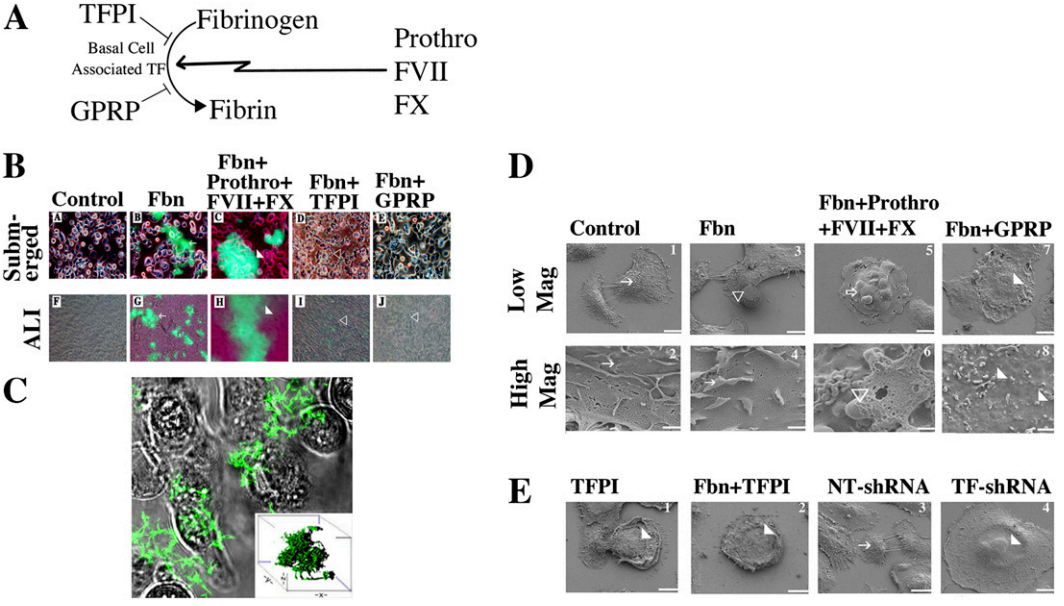

Figure 3. Clotting cascade gene expression and fibrin formation in basal cells. (*A*) To determine if basal cell–associated TF mediates fibrin network formation, basal cells were cultured on collagen-coated glass coverslip chambers (submerged monolayers) for 24 hours or on collagen-coated snapwells at the air–liquid interface for 7 days. Cells were treated with TFPI or peptide Gly-Pro-Arg-Pro (GPRP) for 30 minutes before addition of FITC-fibrinogen (Fbn) and $CaCl_2$ or FITC-fibrinogen, prothrombin (prothro), Factor VII (FVII), Factor X (FX), and $CaCl_2$. Cells were incubated for 30 minutes, and fibrin network (*green*) formation was evaluated using a fluorescence microscope. *Arrows* indicate fibrin networks, *white arrowheads* indicate large fibrin networks, and *open arrowheads* indicate areas without fibrin networks. (*B*) Fibrin network formation under various conditions. (*A–E*) Submerged cultures. (*F–J*) Air–liquid interface cultures. Treatment conditions: *A* and *F*, controls; *B* and *G*, Fbn; *C* and *H*, Fbn+Prothro+FVII+FX; *D* and *I*, Fbn+TFPI; *E* and *J*, Fbn+GPRP. (*C*) Confocal microscopy of fibrin networks formed by submerged basal cells treated with FITC-fibrinogen and $CaCl_2$ in HBSA for 30 minutes (please see online supplement). A merge of the differential interference contrast (transmitted light) and green fluorescence image is shown. *Inset* shows a three-dimensional reconstruction of fibrin network. A video demonstrating the *z* stacks is shown in online supplement (Figure 3 video1.mov). (*D*) Scanning electron microscopic analysis of fibrin networks on the surface of basal cells. Basal cells were cultured on collagen-coated glass coverslips for 24 hours and treated with diluent, GPRG, or TFPI for 30 minutes. A second set of cultures was grown on collagen-coated plastic and transduced with nontarget or TF shRNA for 24 hours. Cultures were then treated with $CaCl_2$ in HBSA and various additives: no factors (control); fibrinogen (Fbn); or Fbn, prothrombin (prothro), Factor VII (FVII), Factor X (FX, 1 nM). Cells were then fixed and processed for scanning electron microscopy. Low magnification (mag) images of basal cells treated with agent(s) indicated at the top of each column. Low Mag: ×2,000; *scale bar* = 10 μm. High Mag: ×25,000; *scale bar* = 1 μm. *White arrows*, tight network fibrin fibers on cell; *white arrowheads*, smooth cell surface; *open arrowheads*, fibrin networks of fibrin formed from exogenously added fibrinogen; *open arrows*, larger fibrin aggregates. (*E*) Scanning electron microscopy analysis of fibrin upon TF inhibition using TFPI and TF shRNA in basal cells. *Arrows* as indicated in *D*. *Scale bar* = 10 μm.

TF-initiated conversion of fibrinogen to fibrin was enhanced by added coagulation factors and was dependent on active TF. The location of the fibrin network was examined by confocal microscopy. Incubation of basal cells with FITC-conjugated fibrinogen in serum-free medium caused formation of dense fibrin networks (Figure 3C, and *see* video 1.mov in the online supplement). Fibrin network formation was inhibited by the thrombin inhibitors (hirudin and PPACK) and indicated that this process required thrombin (not shown). Finally, fibrin networks required calcium and were fully inhibited by 1 mM EDTA (not shown). Thus, TF-mediated formation of fibrin networks occurred at the basal cell surface.

Ultrastructural Characteristics of the Fibrin Network

To evaluate cell surface fibrin networks in greater detail, basal cell surfaces were examined by scanning electron microscopy. In control basal cells grown in serum-free medium, ruffled fibrin filaments were detected (Figure 3D, *panels 1* and *2*). These extended to neighboring cells and covered surfaces of untreated control cells. Cells treated with fibrinogen had larger, thicker fibrin networks that frequently formed floating spheres (Figure 3D, *panels 3* and *4*). The addition of Factor VII, Factor X, and prothrombin resulted in more extensive networks (Figure 3D, *panels 5* and *6*). Under these conditions, the cell surface appeared to be more ruffled and was coated with thicker fibrin filaments. Treatment with cross-linking inhibitor GPRP decreased fibrin filament density (Figure 3D, *panels 7* and *8*), and the diminished networks resembled shortened stalks (more images in Figure E6). Thus, basal cells formed fibrin networks at their surfaces, the extent and complexity of which were increased by the addition of coagulation cascade factors and components.

To determine if TF activity was necessary for fibrin network formation, basal cells were treated with TFPI and evaluated by scanning electron microscopy. TFPI decreased fibrin network formation and resulted in a smoother cell surface (Figure 3D, *panels 1* and *2*). Knockdown of TF by shRNA decreased fibrin network relative to cells transfected with nontarget shRNA (Figure 3E, *panels 3* and *4*). Thus, basal cell–derived TF expression and activity are required for cell surface fibrin network formation.

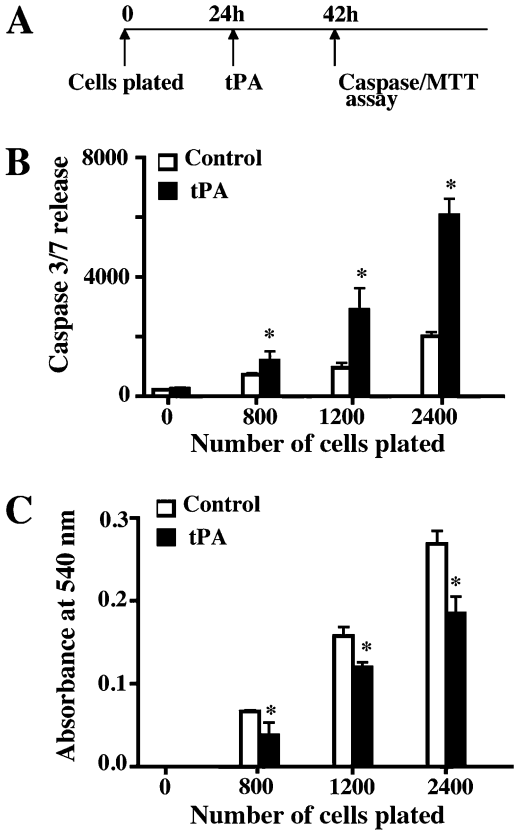

Figure 4. The fibrin network is necessary for basal cell survival. (*A*) Basal cells were allowed to adhere for 24 hours and then treated for 18 hours with diluent or tissue plasminogen activator (tPA). Apoptosis and cell number were assayed. (*B*) Caspase 3/7 activity was measured in culture medium and using Caspase-Glo 3/7 assay. Caspase 3/7 release indicates luminescence (in relative luminescence units) with the background signal subtracted. *White bars*, control (diluent); *black bars*, tPA. (*C*) Cell number was determined using the MTT assay. *White bars*, control (diluent); *black bars*, tPA. Each data set represents three independent experiments performed with cells isolated from three different donors. Data are presented as mean ± SEM ($n = 8$). *$P < 0.05$ for diluent versus tPA.

Fibrin Network Formation Is Necessary for Basal Cell Survival

To further determine if fibrin network was necessary for basal cell survival, cells were allowed to adhere for 24 hours and treated with diluent or tissue-type plasminogen activator (tPA) (Figure 4A). tPA is a serine protease that is found in a variety of mammalian tissues, including airway epithelial cells (30). It converts plasminogen to plasmin, which is a key activity involved in fibrinolysis. Caspase 3/7 release and cell number were measured 18 hour after tPA treatment. tPA treatment increased apoptosis (Figure 4B) and decreased cell number (Figure 4C) at each cell input. The extent of cell death induced by tPA was similar to that caused by TFPI, as shown by experiments that used an equivalent basal cell to tPA molecule ratio to those used in studies involving TFPI-induced cell death (1:7 for TFPI and 1:9 for tPA at 280 nM) (Figures E7A and E7B). We also used Gly-Pro-Arg-Pro (GPRP), a peptide inhibitor of fibrin cross-linking, to further assess the role of fibrin network in basal cell survival. Treatment with GPRP enhanced basal cell apoptosis and decreased proliferation (not shown). The loss of cell viability by disruption of fibrin network using tPA and/or GPRP confirmed that TF-mediated formation of cell surface fibrin networks promoted basal cell survival.

TF Activates Protease-Activated Receptors Isoforms 1 and 2, Allowing Basal Cell Survival

TF also activates protease-activated receptor isoforms 1 and 2 (PAR1 and PAR2) (31). PAR1 and PAR2 expression in airway epithelial cells has been described (32). We confirmed expression of PAR1 and PAR2 mRNAs in basal cells by qRT-PCR analysis (Figure 5A). These were not significantly modified by scratch injury (Figures 5B and 5E).

PARs mediate their effects by mobilizing cytosolic calcium. We used PAR1 and PAR2 peptide antagonists and the cytosolic calcium-sensing dye Fluo-4AM to determine if basal cells expressed active PAR1 and PAR2. Treatment with the PAR1 antagonist 3-mercaptopropionyl-F-Cha-Cha-RKNDK-NH2 or with the PAR2 antagonist FSLLRY-NH2 demonstrated that basal cells expressed active PAR1 (Figures 5C and 5D) and PAR2 (Figures 5F and 5G). To determine if baseline basal cell PAR1 or PAR2 could be activated further, we treated basal cells with PAR1 agonist TFLLRN or PAR2 agonist SLIGRL-NH2. Both stimulated calcium mobilization (Figures 5C, 5D, 5F, and 5G). Agonist-induced PAR1 activity was specifically inhibited by PAR1 antagonist and partially inhibited by PAR2 antagonist. Similarly, agonist-induced PAR2 activity was inhibited by the PAR2 antagonist and partially inhibited by

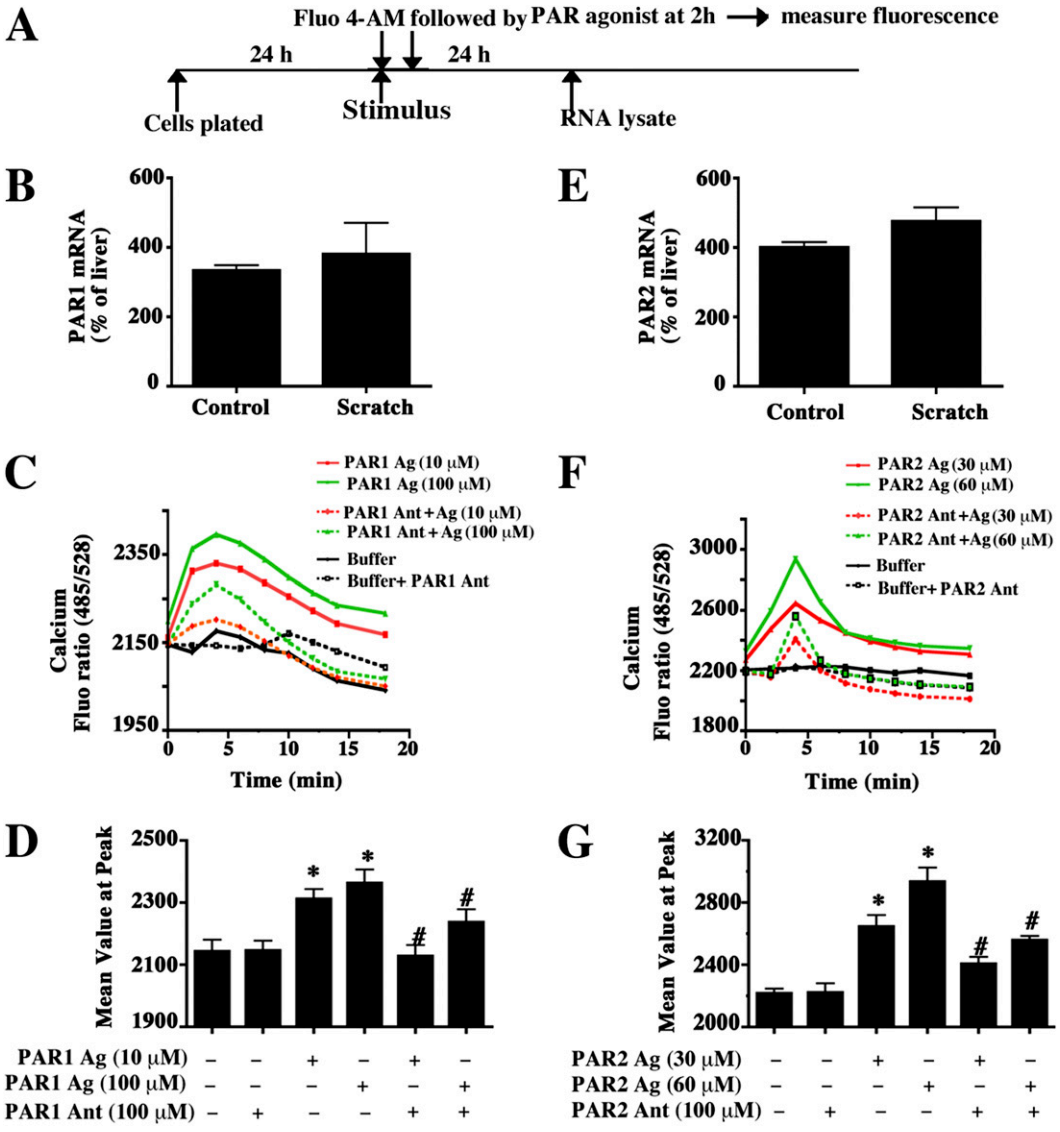

Figure 5. Expression and activity of protease-activated receptors (PAR1 and PAR2) in basal cells. (*A*) Passage 1 basal cells were allowed to adhere to collagen-coated plates for 24 hours. One set of cultures was mechanically injured using a pipette tip (scratch stimulus to observe potential induction), and all cultures were incubated for 24 hours, followed by total RNA recovery. An additional set of cultures was loaded with the cytosolic calcium–sensing dye Fluo-4AM and then treated with PAR agonist or antagonist for 2 hours. Calcium flux was then measured. (*B* and *E*) Expression of PAR1 (*B*) and PAR2 (*E*) mRNA was determined by quantitative RT-PCR. Individual mRNAs were normalized to 18S rRNA, and fold change relative to human liver mRNA (a positive control) was calculated. Data are presented as the mean ± SEM ($n = 3$). (*C* and *F*) The time course for cytosolic calcium mobilization under various treatment conditions. (*C*) PAR1 agonist (Ag, 10 or 100 μM TFLLRN) and PAR1 antagonist (Ant 100 μM, 3-mercaptopropionyl-F-Cha-Cha-RKNDK-amide). (*F*) PAR2 agonist (30 or 60 μM of SLIGRL-NH2) and PAR 2 antagonist (100 μM, FSLLRY-Amide). (*D* and *G*) The mean peak values for the curves presented in *C* and *F*, respectively. Data are presented as the mean ± SEM ($n = 3$). *$P <$ 0.05 for buffer versus treated cells.

the PAR1 antagonist. Thus, basal cells expressed active PARs, and their baseline activity was submaximal.

To determine if active TF was necessary for PAR activation, basal cells were attached for 24 hours, loaded with Fluo-4-AM, and treated with diluent or TFPI (30 min). Agonist-mediated PAR activities were assayed 30 minutes later (Figure 6A). TFPI completely inhibited agonist-mediated PAR1- or PAR2-dependent cytosolic calcium mobilization (Figure 6B). To determine if agonist or antagonist-treated cells were viable and if PAR inhibition was specific, ATP-induced cytosolic calcium signaling was evaluated. This response was unaffected upon TF inhibition (not shown). These data indicated that active TF was necessary for PAR1 and PAR2 activation.

TF Functions Upstream of PAR1 and PAR2 to Promote Basal Cell Survival

The previous data sets indicated that TF activated coagulation and PAR1/2. To determine the order in which these two pathways functioned, we first determined if pretreatment with PAR agonists or antagonists could overcome the TFPI-mediated decrease in basal cell survival and number. Basal cells were adhered for 24 hours and treated with PAR agonists or antagonists for 8 hours. Cells were then treated with diluent or TFPI apoptosis, and cell number was assayed 18 hours after treatment (Figure 6C). TFPI treatment increased apoptosis as indicated by caspase 3/7 release (Figure 6D). Prior agonist-mediated activation of PAR1 or PAR2 reversed TFPI-mediated apoptosis. Similar results were obtained when basal cells were incubated with a combination of PAR1 and PAR2 agonists (not shown). These data indicated that TF functioned upstream of PAR1 and PAR2.

We next evaluated the effect of diluent/TFPI after antagonism of PAR1 or PAR2. Inhibition of PAR1 or PAR2 by their antagonists did not alter TFPI-induced caspase release (Figure 6D). However, antagonist treatment followed by TFPI treatment increased caspase release 2.5-fold (Figure 6D). The basal levels of caspases may be nonspecific, pertinent to the culture system and methods, and not affected by PARs. The additive effect of PAR antagonism and TF inhibition suggested that TF functioned in two processes—PAR activation and fibrin network formation—and that the function of both pathways was necessary for basal cell survival.

We then determined if pretreatment with PAR agonists or antagonists overcame the TFPI-induced decrease in basal cell proliferation. As indicated, basal cells were treated with agonist or antagonist followed by diluent or TFPI. Cell survival was determined using MTT assay 18 hours later (Figure 6E). As shown

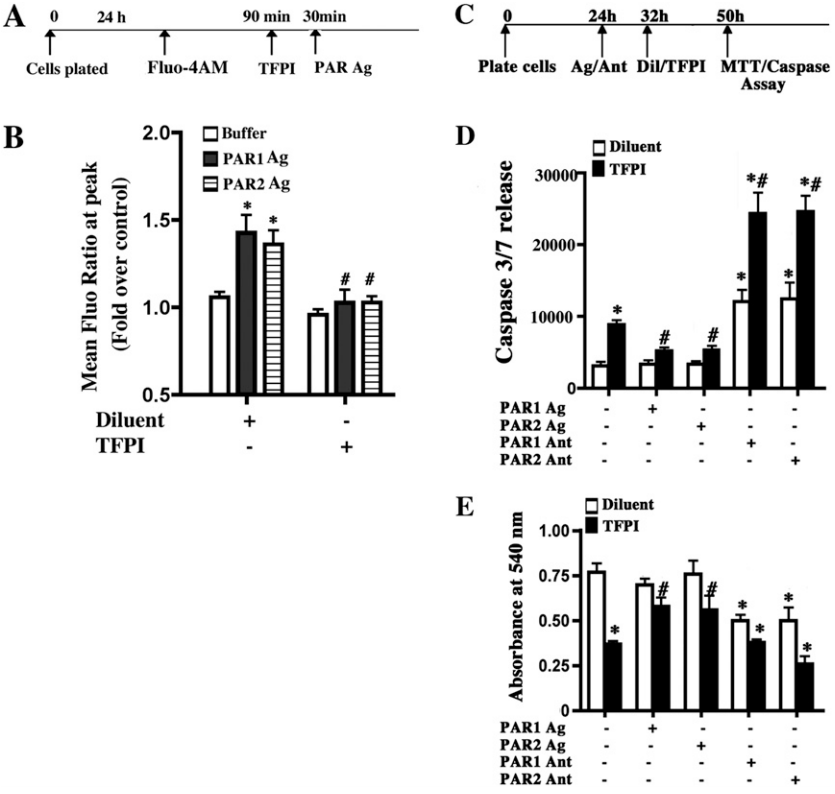

Figure 6. Basal cell–associated TF is necessary for PAR1 and PAR2 activity and functions upstream of PAR1 and PAR2 to promote basal cell survival. (*A*) Basal cells were grown to confluence on collagen-coated, clear–bottom, black-walled, 96-well plates. Cells were loaded with cytosolic calcium–sensing dye Fluo-4AM Cells for 90 minutes and then incubated with diluent or TFPI for 30 minutes. Cells were then stimulated with buffer or agonist. The PAR1 agonist (PAR1 Ag) was TFLLRN, and the PAR 2 agonist (PAR2 Ag) was FSLLRY-amide. (*B*) PAR activity. The mean peak Fluor-4AM (Fluo) value and fold change relative to control were determined. Each data set represents three independent experiments performed with cells isolated from three different donors. Data are presented as mean ± SEM ($n = 3$). $^{*}P < 0.05$ for buffer versus agonist treatment. $^{\#}P < 0.05$ for buffer versus TFPI and agonist. (*C*) Basal cells were allowed to adhere for 24 hours and treated with PAR agonists (Ag) (PAR1: TFLLRN; PAR: 2 FSLLRY-amide) or antagonists (Ant) (PAR 1: 3-mercaptopropionyl-F-Cha-Cha-RKNDK-amide; PAR 2: antagonist FSLLRY-amide) for 8 hours. Cells were then treated with diluent or TFPI, and caspase release or cell number were measured 18 hours later. (*D*) Caspase 3/7 activity was measured in culture medium and using the Caspase-Glo 3/7 assay. Caspase 3/7 release indicates luminescence with background signal subtracted. *White bar*, diluent; *black bar*, TFPI. (*E*) Cell number was evaluated using MTT. *White bar*, diluent; *black bar*, TFPI. Each data set represents three independent experiments performed with cells isolated from three different donors. Data are presented as mean ± SEM ($n = 3$). $^{*}P < 0.05$ for comparisons to untreated control. $^{\#}P > 0.05$ for comparisons to TFPI-treated control.

previously, TFPI-treatment decreased basal cell number relative to vehicle treatment (Figure 6E). Prior activation of PAR1 or PAR2 receptors by their respective agonists prevented the TFPI-mediated decrease in cell number. Preinhibition of PAR1 or PAR2 by treatment with their respective antagonists resulted in decreased basal cell number. This effect was exaggerated by TFPI treatment. We also evaluated if PAR activation protected against TF knockdown–induced basal cell apoptosis. PAR activation significantly decreased caspase release in TF-shRNA–transduced basal cells (Figure E8). These data also supported the conclusion that TF played a role in multiple basal cell survival pathways.

TF-Dependent Fibrin Network Formation and PAR Activation Cooperate To Promote Basal Cell Survival

To determine if TF-dependent activation of coagulation and of PAR receptors occurred in parallel or sequence, basal cells were adhered for 24 hours and treated with PAR1 or PAR2 antagonist. Two hours later, fibrin networks were evaluated in the presence of fibrinogen and calcium chloride (Figures E9B, E9E, and E9H). Fibrin network formation was not altered by PAR1 or PAR2 antagonism. Similarly, the extensive fibrin network that formed in the presence of added prothrombin, Factor VII, and Factor X was not altered by PAR inhibition (Figures E9C, E9F, and E9I). These data suggested that the basal cell–associated TF functioned as part of two distinct cascades: (*1*) PAR1 and PAR2 activation and (*2*) initiation of coagulation (Figure 7).

DISCUSSION

The purpose of this study was to determine the impact of TF-dependent coagulation and PAR activation on basal cell survival. Cell surface TF-dependent coagulation was previously demonstrated in the human lung, transformed tracheal epithelial cells, and bronchial epithelial cells or cell lines (19, 33). Antibodies against TF, fibrinogen, and FXIIIa inhibited repair (19). Despite these important findings, their significance has not been extended beyond those in transformed or malignant cells.

TF is a marker for nasal and embryonic basal cells (16–18). We showed that all first-passage human tracheobronchial epithelial cells were keratin 5–positive basal cells that also expressed TF. Thus, TF is also a marker for tracheobronchial basal cells. Basal cells play dual roles in airways by attaching epithelium to the airways and by serving as stem or progenitor cells (16, 34–36). Tracheobronchial basal cells can restore a fully differentiated epithelium *in vitro* (16, 36). TF-expressing basal cells from nasal airways had several-fold greater colony forming ability than TF-negative columnar epithelial cells (16). Thus, TF expression in human tracheal basal cells may have critical functions beyond coagulation.

We showed that basal cell–associated TF was active, whereas TF activity was regulated by the availability of coagulation cascade factors VII and X. Our data contrast with those from bronchial epithelial cell lines wherein mechanical injury caused fibrin matrix formation and rapid generation of FVII, VX, FXIIIa, D-dimers, fibrinogen, and soluble fibrin. These data suggest that an important difference between primary basal cell isolates and cell lines is the selection of cells that express a more complete spectrum of preformed coagulation proteins (19). The limited detectability of some of the clotting factors, such as FVII in primary basal cell isolates, could be due to short mRNA half-lives (37). However, our functional assays and kinetic analyses indicate that basal cell–associated TF activity is dependent on added FVII and FX. The present study suggests that human tracheobronchial basal cells contribute to fibrin formation, but this activity is dependent upon additional plasma-derived factors. This codependence may be critical to regulate fibrin formation in airways such that this does not occur except when vascular integrity is compromised.

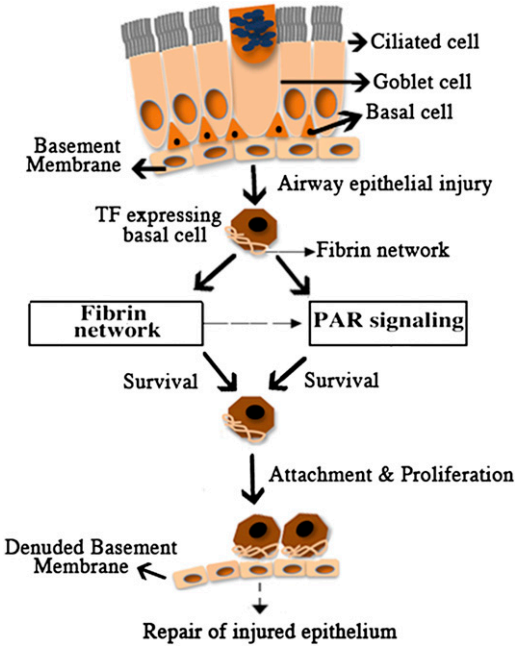

Figure 7. Roles played by TF in basal cell survival. Schematic representation of TF-mediated fibrin network formation and PAR activation providing basal cell survival attachment and proliferation to potentially restore injured airway epithelium.

We found that TF inhibition caused extensive basal cell apoptosis and necrosis. Thus, TF affects cell functions that may not be related to TF's clotting function. The TF–FVIIa complex is known to activate PARs, promoting cell survival and proliferation (38). The antiapoptotic role of TF was demonstrated previously in TF-positive BHK cells where FVIIa binding to TF protected against apoptosis induced by growth factor deprivation (39). The TF/FVIIa complex in another study also activated antiapoptotic proteins like Bcl2, and TF inhibition enhanced apoptotic cell death in certain tumor cells (40). Furthermore, TF overexpression in cardiomyocytes protected against TNF-induced apoptosis (41). By contrast, TF inhibition via TFPI also caused FAS ligand–mediated apoptotic cell death in macrophages (42). In vascular smooth muscle cells, TFPI induction caused inhibition of proliferation and enhanced apoptosis (43). Although TF-mediated fibrin deposition and consequent pathogenesis of airway disease has been reported, we now establish a role of TF in promoting airway epithelial cell and basal cell survival.

We showed that TF was necessary to form basal cell–associated fibrin networks. Indeed, fibrin network formation by blood vessel–associated cell types has been previously noted. For example, cell surface fibrin formation from exogenously added fibrinogen was found in fibroblasts, where thrombin, FVII, and FX additives were required (22). TF expression and fibrin on smooth muscle cell surfaces promotes proliferation via a thrombin- and PAR-dependent mechanism (44). Although human bronchial epithelial cell line 16HBE can up-regulate fibrinogen upon wounding, direct demonstration of fibrin network formation by primary basal cells is a new finding. This study is also unique in using scanning electron microscopy to demonstrate TF-dependent fibrin networks on basal cell surfaces. Inhibition by GPRP confirmed that the ruffled structure on epithelial cell surfaces was fibrin. In sum, human airway epithelial basal cells support formation of fibrin networks on their surfaces, and this process favors proliferation.

Given the role of PARs in coagulation-dependent signaling, we suspected that PARs might be active in basal cells. PARs contribute to tissue responses to injury, including repair and cell survival (45). PARs are widely expressed within the respiratory tract, and PAR1 and PAR2 are the dominant isoforms in tracheal epithelium (46). Previous studies suggested that PARs are important in downstream TF-dependent effects (47). We report here that TF was necessary for optimal PAR1 and PAR2 activity.

This study indicates that PARs confer prosurvival and proproliferative effects of TF. PAR1 and PAR2 activation, via ligand binding, may also activate TF (27). Thus, PAR signaling may "self-amplify" or feed forward. Binding of TF to FVIIa activates PARs and regulates prosurvival proteins, thereby influencing proliferation and survival (48). Binding of active Factor VII causes cytosolic calcium mobilization and signal transduction via mitogen-activated protein kinase phosphorylation (49). Factor VII–dependent PAR1 signaling promotes barrier function in endothelium (50). PAR2 can also be protective against virus-induced lung injury (51). By contrast, PAR2-dependent increases in TF-dependent fibrin formation and myofibroblast differentiation may promote pulmonary fibrosis (52). Here we report that PARs confer the prosurvival and proproliferative effects of TF in airway epithelial basal cells. Downstream signaling and procoagulant effects seem to be required. Because TF, fibrin networks, and PAR activation were important for basal cell proliferation, we suggest that TF mediates basal cell attachment and survival, leading to proliferation (Figure 7). We propose, therefore, that TF activity contributes to repair of mucosal surfaces by promoting extravascular provisional fibrin matrix formation, allowing survival and proliferation of airway epithelial basal cells.

These data may indicate a new direction for tissue engineering in the large airways. Recent studies indicated that fibrin gels can be used to form or reinforce cellular scaffolds, control release and delivery of gene therapy, slowly release and deliver growth factors, and store and/or deliver cell-based therapies (53). Fibrin can direct cell migration and homing of circulation-derived cells and may direct proliferation, differentiation, and gene expression (54, 55). The current study enhances our understanding of the potential utility of fibrin in the regeneration or replacement of large airway epithelium and advances a TF-centered approach to scaffolds, provisional matrices, and cell-based treatment of large airways.

Author disclosures are available with the text of this article at www.atsjournals.org.

Acknowledgments: The authors thank Dr. Alisa Wolberg for many very useful discussions and for providing FITC-labeled fibrinogen for the studies and Abhilasha Jain, Stacy Miller, Jenai Kailey, Rhonda Garlick, and Russell Smith for excellent technical assistance. FLOW cytometry analysis was conducted at the University of Colorado Cancer Center Flow Core.

References

1. Rao LV, Mackman N. Factor VIIa and tissue factor: from cell biology to animal models. *Thromb Res* 2010;125:S1–S3.
2. Fan L, Yotov WV, Zhu T, Esmailzadeh L, Joyal JS, Sennlaub F, Heveker N, Chemtob S, Rivard GE. Tissue factor enhances protease-activated receptor-2-mediated factor VIIa cell proliferative properties. *J Thromb Haemost* 2005;3:1056–1063.
3. Idell S. Coagulation, fibrinolysis, and fibrin deposition in acute lung injury. *Crit Care Med* 2003;31:S213–S220.
4. Bastarache JA, Wang L, Geiser T, Wang Z, Albertine KH, Matthay MA, Ware LB. The alveolar epithelium can initiate the extrinsic coagulation cascade through expression of tissue factor. *Thorax* 2007;62:608–616.
5. Wygrecka M, Markart P, Fink L, Guenther A, Preissner KT. Raised protein levels and altered cellular expression of factor VII activating protease (FSAP) in the lungs of patients with acute respiratory distress syndrome (ARDS). *Thorax* 2007;62:880–888.
6. Bastarache JA, Fremont RD, Kropski JA, Bossert FR, Ware LB. Procoagulant alveolar microparticles in the lungs of patients with acute

respiratory distress syndrome. *Am J Physiol Lung Cell Mol Physiol* 2009;297:L1035–L1041.
7. Bastarache JA, Wang L, Wang Z, Albertine KH, Matthay MA, Ware LB. Intra-alveolar tissue factor pathway inhibitor is not sufficient to block tissue factor procoagulant activity. *Am J Physiol Lung Cell Mol Physiol* 2008;294:L874–L881.
8. Veress LA, O'Neill HC, Hendry-Hofer TB, Loader JE, Rancourt RC, White CW. Airway obstruction due to bronchial vascular injury after sulfur mustard analog inhalation. *Am J Respir Crit Care Med* 2010; 182:1352–1361.
9. Rancourt RC, Veress LA, Guo X, Jones TN, Hendry-Hofer TB, White CW. Airway tissue factor-dependent coagulation activity in response to sulfur mustard analog 2-chloroethyl ethyl sulfide. *Am J Physiol Lung Cell Mol Physiol* 2011;302:L82–L92.
10. Enkhbaatar P, Murakami K, Cox R, Westphal M, Morita N, Brantley K, Burke A, Hawkins H, Schmalstieg F, Traber L, *et al.* Aerosolized tissue plasminogen inhibitor improves pulmonary function in sheep with burn and smoke inhalation. *Shock* 2004;22:70–75.
11. Heath L, Ling S, Racz J, Mane G, Schmidt L, Myers JL, Tsai WC, Caruthers RL, Hirsch JC, Stringer KA. Prospective, longitudinal study of plastic bronchitis cast pathology and responsiveness to tissue plasminogen activator. *Pediatr Cardiol* 2011;32:1182–1189.
12. Monroe DM, Mackman N, Hoffman M. Wound healing in hemophilia b mice and low tissue factor mice. *Thromb Res* 2010;125:S74–S77.
13. Pedersen B, Holscher T, Sato Y, Pawlinski R, Mackman N. A balance between tissue factor and tissue factor pathway inhibitor is required for embryonic development and hemostasis in adult mice. *Blood* 2005; 105:2777–2782.
14. Drake TA, Morrissey JH, Edgington TS. Selective cellular expression of tissue factor in human tissues: implications for disorders of hemostasis and thrombosis. *Am J Pathol* 1989;134:1087–1097.
15. Flossel C, Luther T, Muller M, Albrecht S, Kasper M. Immunohistochemical detection of tissue factor (TF) on paraffin sections of routinely fixed human tissue. *Histochemistry* 1994;101:449–453.
16. Hajj R, Baranek T, Le Naour R, Lesimple P, Puchelle E, Coraux C. Basal cells of the human adult airway surface epithelium retain transit-amplifying cell properties. *Stem Cells* 2007;25:139–148.
17. Imokawa S, Sato A, Hayakawa H, Kotani M, Urano T, Takada A. Tissue factor expression and fibrin deposition in the lungs of patients with idiopathic pulmonary fibrosis and systemic sclerosis. *Am J Respir Crit Care Med* 1997;156:631–636.
18. Hackett TL, Shaheen F, Johnson A, Wadsworth S, Pechkovsky DV, Jacoby DB, Kicic A, Stick SM, Knight DA. Characterization of side population cells from human airway epithelium. *Stem Cells* 2008;26: 2576–2585.
19. Perrio MJ, Ewen D, Trevethick MA, Salmon GP, Shute JK. Fibrin formation by wounded bronchial epithelial cell layers in vitro is essential for normal epithelial repair and independent of plasma proteins. *Clin Exp Allergy* 2007;37:1688–1700.
20. Ahmad S, Ahmad A, Dremina ES, Sharov VS, Guo X, Jones TN, Loader JE, Tatreau JR, Perraud AL, Schoneich C, *et al.* Bcl-2 suppresses sarcoplasmic/endoplasmic reticulum Ca2+-atpase expression in cystic fibrosis airways: role in oxidant-mediated cell death. *Am J Respir Crit Care Med* 2009;179:816–826.
21. Ahmad S, Nichols DP, Strand M, Rancourt RC, Randell SH, White CW, Ahmad A. Serca2 regulates non-CF and CF airway epithelial cell response to ozone. *PLoS ONE* 2011;6:e27451.
22. Campbell RA, Overmyer KA, Bagnell CR, Wolberg AS. Cellular procoagulant activity dictates clot structure and stability as a function of distance from the cell surface. *Arterioscler Thromb Vasc Biol* 2008;28: 2247–2254.
23. Ahmad S, Raemy DO, Loader JE, Kailey JM, Neeves KB, White CW, Ahmad A, Gehr P, Rothen-Rutishauser BM. Interaction and localization of synthetic nanoparticles in healthy and cystic fibrosis airway epithelial cells: effect of ozone exposure. *J Aerosol Med Pulm Drug Deliv* 2012;25:7–15.
24. Ahmad S, Ahmad A, McConville G, Schneider BK, Allen CB, Manzer R, Mason RJ, White CW. Lung epithelial cells release ATP during ozone exposure: signaling for cell survival. *Free Radic Biol Med* 2005;39:213–226.
25. Ahmad S, Ahmad A, Schneider KB, White CW. Cholesterol interferes with the MTT assay in human epithelial-like (A549) and endothelial (HLMVE and HCAE) cells. *Int J Toxicol* 2006;25:17–23.
26. Dorfleutner A, Hintermann E, Tarui T, Takada Y, Ruf W. Cross-talk of integrin alpha3beta1 and tissue factor in cell migration. *Mol Biol Cell* 2004;15:4416–4425.
27. Ahamed J, Ruf W. Protease-activated receptor 2-dependent phosphorylation of the tissue factor cytoplasmic domain. *J Biol Chem* 2004;279: 23038–23044.
28. Key NS, Mackman N. Tissue factor and its measurement in whole blood, plasma, and microparticles. *Semin Thromb Hemost* 2010;36:865–875.
29. Kaczmarek E, Lee MH, McDonagh J. Initial interaction between fibrin and tissue plasminogen activator (t-PA): the gly-pro-arg-pro binding site on fibrin(ogen) is important for t-PA activity. *J Biol Chem* 1993; 268:2474–2479.
30. Idell S, Kumar A, Zwieb C, Holiday D, Koenig KB, Johnson AR. Effects of TGF-beta and TNF-alpha on procoagulant and fibrinolytic pathways of human tracheal epithelial cells. *Am J Physiol* 1994;267: L693–L703.
31. Mackman N, Taubman M. Tissue factor: past, present, and future. *Arterioscler Thromb Vasc Biol* 2009;29:1986–1988.
32. Ostrowska E, Sokolova E, Reiser G. PAR-2 activation and LPS synergistically enhance inflammatory signaling in airway epithelial cells by raising PAR expression level and interleukin-8 release. *Am J Physiol Lung Cell Mol Physiol* 2007;293:L1208–L1218.
33. Shetty S, Bhandary YP, Shetty SK, Velusamy T, Shetty P, Bdeir K, Gyetko MR, Cines DB, Idell S, Neuenschwander PF, *et al.* Induction of tissue factor by urokinase in lung epithelial cells and in the lungs. *Am J Respir Crit Care Med* 2010;181:1355–1366.
34. Boers JE, Ambergen AW, Thunnissen FB. Number and proliferation of basal and parabasal cells in normal human airway epithelium. *Am J Respir Crit Care Med* 1998;157:2000–2006.
35. Evans MJ, Van Winkle LS, Fanucchi MV, Plopper CG. Cellular and molecular characteristics of basal cells in airway epithelium. *Exp Lung Res* 2001;27:401–415.
36. Engelhardt JF, Schlossberg H, Yankaskas JR, Dudus L. Progenitor cells of the adult human airway involved in submucosal gland development. *Development* 1995;121:2031–2046.
37. Prydz H, Gaudernack G. Studies on the biosynthesis of factor VII (proconvertin): the mode of action of warfarin. *Biochim Biophys Acta* 1971;230:373–380.
38. van den Hengel LG, Versteeg HH. Tissue factor signaling: a multifaceted function in biological processes. *Front Biosci* 2011;3:1500–1510. (Schol Ed).
39. Sorensen BB, Rao LV, Tornehave D, Gammeltoft S, Petersen LC. Antiapoptotic effect of coagulation factor VIIa. *Blood* 2003;102:1708–1715.
40. Fang J, Tang H, Xia L, Zhou M, Chen Y, Wei W, Hu Y, Song S, Hong M. Down-regulation of tissue factor by siRNA increased doxorubicin-induced apoptosis in human neuroblastoma. *J Huazhong Univ Sci Technolog Med Sci* 2008;28:42–45.
41. Boltzen U, Eisenreich A, Antoniak S, Weithaeuser A, Fechner H, Poller W, Schultheiss HP, Mackman N, Rauch U. Alternatively spliced tissue factor and full-length tissue factor protect cardiomyocytes against TNF-alpha-induced apoptosis. *J Mol Cell Cardiol* 2012;52:1056–1065.
42. Pan JJ, Shi HM, Luo XP, Ma D, Li Y, Zhu J, Liang W, Mu JG, Li J. Recombinant TFPI-2 enhances macrophage apoptosis through upregulation of FAS/FASL. *Eur J Pharmacol* 2011;654:135–141.
43. Ekstrand J, Razuvaev A, Folkersen L, Roy J, Hedin U. Tissue factor pathway inhibitor-2 is induced by fluid shear stress in vascular smooth muscle cells and affects cell proliferation and survival. *J Vasc Surg* 2010;52:167–175.
44. Marutsuka K, Hatakeyama K, Sato Y, Yamashita A, Sumiyoshi A, Asada Y. Protease-activated receptor 2 (PAR2) mediates vascular smooth muscle cell migration induced by tissue factor/factor VIIa complex. *Thromb Res* 2002;107:271–276.
45. Ossovskaya VS, Bunnett NW. Protease-activated receptors: contribution to physiology and disease. *Physiol Rev* 2004;84:579–621.
46. Lan RS, Stewart GA, Henry PJ. Role of protease-activated receptors in airway function: a target for therapeutic intervention? *Pharmacol Ther* 2002;95:239–257.
47. Camerer E, Huang W, Coughlin SR. Tissue factor- and factor X-dependent activation of protease-activated receptor 2 by factor VIIa. *Proc Natl Acad Sci USA* 2000;97:5255–5260.
48. Versteeg HH, Ruf W. Emerging insights in tissue factor-dependent signaling events. *Semin Thromb Hemost* 2006;32:24–32.

49. Poulsen LK, Jacobsen N, Sorensen BB, Bergenhem NC, Kelly JD, Foster DC, Thastrup O, Ezban M, Petersen LC. Signal transduction via the mitogen-activated protein kinase pathway induced by binding of coagulation factor VIIa to tissue factor. *J Biol Chem* 1998;273:6228–6232.
50. Sen P, Gopalakrishnan R, Kothari H, Keshava S, Clark CA, Esmon CT, Pendurthi UR, Rao LV. Factor VIIa bound to endothelial cell protein C receptor activates protease activated receptor-1 and mediates cell signaling and barrier protection. *Blood* 2011;117:3199–3208.
51. Khoufache K, LeBouder F, Morello E, Laurent F, Riffault S, Andrade-Gordon P, Boullier S, Rousset P, Vergnolle N, Riteau B. Protective role for protease-activated receptor-2 against influenza virus pathogenesis via an IFN-gamma-dependent pathway. *J Immunol* 2009;182:7795–7802.
52. Borensztajn K, Bresser P, van der Loos C, Bot I, van den Blink B, den Bakker MA, Daalhuisen J, Groot AP, Peppelenbosch MP, von der Thusen JH, *et al.* Protease-activated receptor-2 induces myofibroblast differentiation and tissue factor up-regulation during bleomycin-induced lung injury: otential role in pulmonary fibrosis. *Am J Pathol* 2010;177: 2753–2764.
53. Ahmed TA, Dare EV, Hincke M. Fibrin: a versatile scaffold for tissue engineering applications. *Tissue Eng Part B Rev* 2008;14:199–215.
54. de Boer HC, Verseyden C, Ulfman LH, Zwaginga JJ, Bot I, Biessen EA, Rabelink TJ, van Zonneveld AJ. Fibrin and activated platelets cooperatively guide stem cells to a vascular injury and promote differentiation towards an endothelial cell phenotype. *Arterioscler Thromb Vasc Biol* 2006;26:1653–1659.
55. Langer HF, May AE, Vestweber D, De Boer HC, Hatzopoulos AK, Gawaz M. Platelet-induced differentiation of endothelial progenitor cells. *Semin Thromb Hemost* 2007;33:136–143.